DYNAMIC BEHAVIOR AND EXPERIMENTAL VALIDATION OF CELL NUCLEATION AND GROWING MECHANISM IN MICROCELLULAR INJECTION MOLDING PROCESS

Tai-Yi Shiu[1], Yuan-Jung Chang[1], Chao-Tsai Huang[1], David Hsu[1], Rong-Yu Chang[2]

[1] CoreTech System (Moldex3D) Co., Ltd., Hsinchu, Taiwan, R.O.C.
[2] Department of Chemical Engineering, National Tsing Hua University, Hsinchu, Taiwan, R.O.C.

Abstract

We present the recent development of three-dimensional prediction of dynamic behavior of cell nucleation and growing mechanism, and the effect of nucleation-growing competition in microcellular injection molding process. Simulations of microcellular foaming process of injection molding are carried out for polyolefins with supercritical fluids (SCFs) carbon dioxide and nitrogen. In addition, we validate simulation results with experimental results to prove the capability of 3D prediction of microcellular foaming process and further compare simulations of microcellular injection molding and conventional molding to provide insights and economic guidance into design and manufacturing of injection molding products.

Introduction

Microcellular technology has been enormously developing and applied in many foaming processes for many polymers in industrial manufacturing, since the microcellular batch processing technology has brought out by Dr. Nam Suh and co-workers at MIT in the early 1980s [1]. The microcellular application used in reciprocating screw injection molding machine was built by Trexel and Engel in 1998 [2].

Despite the microcellular technology has been developing for more than a decade and widely been used in today's plastic product manufacturing, the reliable computer aided engineering application is not well developed due to limited understanding of complex foaming mechanism. Venerus [3] reviewed numerous diffusion-controlled modeling studies of polymer foaming and showed the diffusion-induced bubble growth in viscoelastic liquids numerically having good agreement with experimental data. Taki [4] studied the effects of pressure release rate on bubble density and sizes. This study applies the well developed models of cell foaming to couple with 3D flow motion technology for microcellular injection molding. The validation of 3D modeling is to compare the experimental data done by Turng and co-workers [5].

Numerical Modeling

The details of several model developments can be found in the papers by Taki [4]. We consider the single phase fluid is of binary constitution, SCFs dissolved in polymer melt, before onset of bubble nucleation. The polymer melt is assumed as General Newtonian Fluid (GNF). Hence the non-isothermal 3D flow motion can be mathematically described by the following:

$$\frac{\partial \rho}{\partial t} + \nabla \cdot \rho \mathbf{u} = 0 \tag{1}$$

$$\frac{\partial}{\partial t}(\rho \mathbf{u}) + \nabla \cdot (\rho \mathbf{u}\mathbf{u} - \boldsymbol{\sigma}) = \rho \mathbf{g} \tag{2}$$

$$\boldsymbol{\sigma} = -p\mathbf{I} + \eta\left(\nabla \mathbf{u} + \nabla \mathbf{u}^T\right) \tag{3}$$

$$\rho C_P\left(\frac{\partial T}{\partial t} + \mathbf{u} \cdot \nabla T\right) = \nabla \cdot (\mathbf{k} \nabla T) + \eta \dot{\gamma}^2 \tag{4}$$

where $\mathbf{u}$ is the velocity vector, T is the temperature, t is the time, p is the pressure, $\boldsymbol{\sigma}$ is the total stress tensor, ρ is the density, η is the viscosity, $\mathbf{k}$ is the thermal conductivity, Cp is the specific heat and $\dot{\gamma}$ is the shear rate. The Finite Volume Method (FVM) due to its robustness and efficiency is employed in this study to solve the transient flow field in complex three-dimensional geometry.

The microcellular foaming process happens after melt is injected into mold cavity. The 3D numerical simulation is applied for describing dynamic behavior of bubble growth which is coupled with macroscopic molten polymer flow. Radius of bubble growth is given as:

$$\frac{dR}{dt} = \frac{R}{4\eta}\left(P_D - P_C - \frac{2\gamma}{R}\right) \tag{5}$$

where bubble radius is R, viscosity is η, bubble pressure

is P_D, ambient pressure is P_C, and surface tension is γ. Thin boundary layer condition is assumed and dissolved gas concentration profile along the radial direction of thin shell is described by a diffusion equation as shown below.

$$\frac{\partial c}{\partial t} = D\left[\frac{1}{r^2}\frac{\partial}{\partial r}\left(r^2\frac{\partial c}{\partial r}\right)\right] \tag{6}$$

where c is dissolved gas concentration and D is the diffusion coefficient.

The dynamic bubble growth behavior is described by the mass transfer at the interface of gas bubble, and is proposed by Han and Yoo [6].

$$\frac{d}{dt}\left(P_D R^3\right) = \frac{6D\left(R_g T\right)\left(c_\infty - c_R\right)R}{-1+\left\{1+\frac{2/R^3}{R_g T}\left(\frac{P_D R^3 - P_{D0}R_0^{\,3}}{c_\infty - c_R}\right)\right\}^{1/2}} \tag{7}$$

The concentration has the following relation,

$$\frac{c_\infty - c}{c_\infty - c_R} = \left(1 - \frac{r-R}{\delta}\right)^2 \tag{8}$$

and δ is the concentration boundary thickness.

Bubble nucleation, describe by equation (9), happens due to pressure drop of molten polymer from sprue to mold cavity during filling process. The cell nucleation and bubble growing is a competition mechanism and can be proposed as a classical exponential function which is coupled with a mass conservation of dissolved gas as given in equation (10).

$$J(t) = f_0\left(\frac{2\gamma}{\pi M_w / N_A}\right)^{1/2}\exp\left(-\frac{16\pi\gamma^3 F}{3k_B T\left(\bar{c}(t)/k_H - P_C(t)^2\right)}\right)N_A\bar{c}(t) \tag{9}$$

where f_0 and F are fitting parameters, $\bar{c}$ is average dissolved gas concentration, N_A is Avogadro number, k_b is Boltzmann constant, and M_w is gas molecular weight.

$$\bar{c}(t)V_{L0} = c_0 V_{L0} - \int_0^t \frac{4\pi}{3}R^3\left(t-t',t'\right)\frac{P_D\left(t-t',t'\right)}{R_g T}J(t')V_{L0}dt' \tag{10}$$

where V_{L0} is the volume of polymer matrix.

Simulations are done by a FVM based algorithm developed by Chang and Yang [7]. The validation of 3D modeling of microcellular injection molding simulation is performed on a CAE software Moldex3D theoretically and the simulation results are compared to the experimental results done by Turng and co-workers [5]. In addition, a comparison of simulation of microcellular and conventional injection molding is for illustrating the benefits of using microcellular injection molding process.

Results and Discussion

Calculated average values of cell density and cell size versus dissolved gas amount from middle cross section area of a microcellular injection molded dog-bone sample are compared with experimental data reported by Turng and co-workers [5] as shown in Fig. 1 and Fig. 2. For PP/N_2 system, as illustrated in Fig. 1, the calculated cell size well agrees with experimental data while the calculated density well quantitatively agrees experiment for lower dissolved gas amount and qualitatively agree with experiment for higher gas concentration. For LDPE/N_2 system, as illustrated in Fig. 2, the calculated cell size and cell density are both have good agreement with the experiments.

Simulation results of two dissolved gas concentrations, 0.24wt% and 0.57wt%, for PP/N_2 system of microcellular injection molded dog-bone sample are analyzed for the cell nucleation and bubble growing behaviors. In Fig. 3, cell density distribution of molded part surface ranges from 90 to 140 cells/mm^3, while that of whole molded part is from 17 to 163 cells/mm^3, and average value is about 111 cells/mm^3, which is mean value calculated from nodes. The maximum value appears at the position where pressure driven flow stops flowing and molten polymer starts to fulfill the cavity by cell expansion; also, the minimum value happens at the end of cavity where is last filled by melt. The density distribution of core section of molded part, as shown in Fig. 4, shows close density range as that of surface of molded part. The cell size distribution results are given in Fig. 5 and Fig. 6 for surface and core section respectively. The radius of molded part is from 0.05μm to 77.6μm and the average radius is 50.09μm; so that, one might observe that cells having size smaller 10μm almost appears near the surface (frozen layer). Comparison of Fig. 5 and Fig. 6 also tells the cells near surface, i.e. frozen layer, are much smaller than average cell size, which is the phenomena observed in a real microcellular injection molded part. Calculated results for 0.57 wt% dissolved SCF are illustrated from Fig. 7 to Fig. 10. The density distribution of molded part of 0.57 wt% dissolved SCF is from 2.28×10^3 cells/mm^3 to 5.36×10^3 cells/mm^3 and the average is 3.71×10^3 cells/mm^3; also, size distribution is from 3.0μm to 32.4μm and the average is 19.6μm. In the average sense, higher dissolved SCF concentration gives higher cell density and smaller cell size than that of lower concentration. The phenomena can be interpreted by the competition behavior between cell

nucleation and bubble growing. In addition, lower dissolved SCF gives more uniformed cell size distribution.

The microcellular injection simulation is also applied to simulate a real product to determine the difference to conventional injection molding. The foaming system is PS/N_2. Melt front time result is given in Fig. 11 to determine the flow and foaming pattern. The injected polymer melt flow stops at 90% of cavity filled and foaming fulfills the rest unfilled mold cavity. Fig. 12 and Fig. 13 show the cell size and density distributions of molded part in different cross sections. Lower cell densities and smaller cell sizes are observed near gates. The average cell size is 14.7 μ m and average density is 1.04×10^4 cells/mm^3, those values are corresponding to a microcellular injection molded part [2]. In addition, we compared the simulated results of dimensional distortion between microcellular and conventional molding as illustrated in Fig. 14 and Fig. 15. The result of microcellular injection molding, as shown in Fig. 14, shows better dimensional stability especially in higher cell density and larger cell size region. We consider the area need highly dimensional stability is indicated by red box in Fig. 14 and Fig. 15. The displacement in y-direction is close to zero for microcellular injection molded part; however, that of conventional injection molded product is about 0.5 mm (0.5%). The poor foaming behavior near gate was observed; so that, the results also recommend that the proper gate position design can control the foaming behavior in order to achieve desired part dimension requirement.

Conclusions

This study presents the 3D simulation capability of predicting dynamic behavior for microcellular injection molding process. Good quantitative agreement between simulation and experimental results of cell density distribution and sizes distribution are found for LDPE, although LDPE has lower melt strength and shows bigger error bar of experimental data of cell sizes. Simulation results of microcellular injection molding for nitrogen SCF dissolved in PP show fairly good agreement with experimental data. In the industrial application, the validation of simulation results with experimental data meet the criteria of prediction capability for further application of microcellular injection molding simulation for a complex geometrical product.

We also carried out the comparisons of calculated results for microcellular injection molding and conventional one. The comparison provides an insight into examination of process design and an economic method to mimic microcellular injection molding process.

References

1. N. P. Suh, Hanser/Garden Publications, Cincinnati, Chpter 3 (1996).
2. J. Xu, John Wiley and Sons, New Jersey (2010).
3. Venerus, *Cellular Polymers*, **22**, 9 (2003).
4. K. Taki, *Chemical Engineering Science*, **63,** 3643 (2008).
5. J. Lee and L.-S. Turng et al, *Polymer*, **52**, 1436 (2011).
6. C. D. Han and H. J. Yoo, *Polymer Engineering and Science*, **21**, 518 (1981).
7. R.-Y. Chang and W.-H. Yang, *Int. J. Numer. Meth. Fluids*, **37**, 125 (2001).

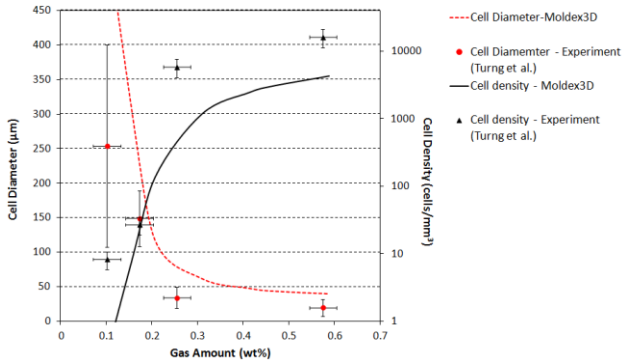

Fig. 1 Comparison of calculated and experimental data of cell sizes and densities for PP/N_2 system. (Y-axis error bar is a guess value of 30% of lowest experimental gas concentration 0.1 wt%)

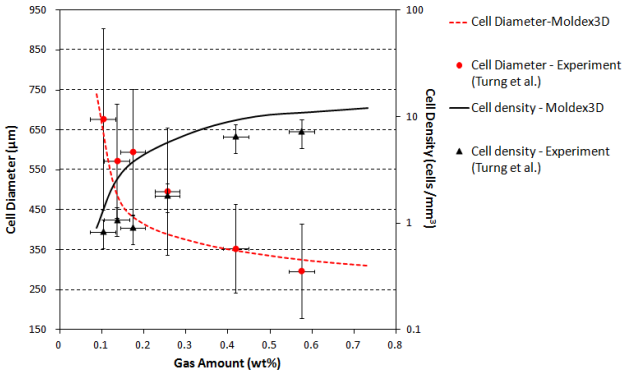

Fig. 2 Comparison of calculated and experimental data of cell sizes and densities for $LDPE/N_2$ system. (Y-axis error bar is a guess value of 30% of lowest experimental gas concentration 0.1 wt%)

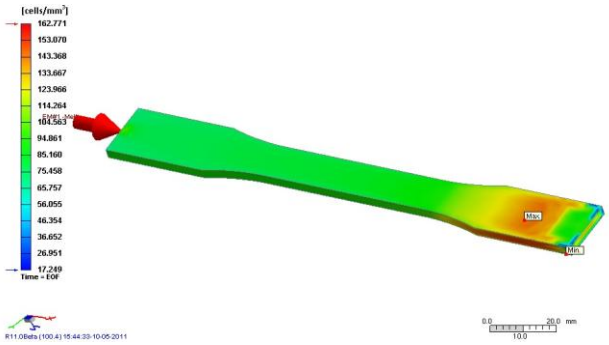

Fig. 3 Cell density distribution of sample surface for 0.24 wt% N_2 SCF dissolved in PP. (Legend scale is 17~163 cells/mm^3)

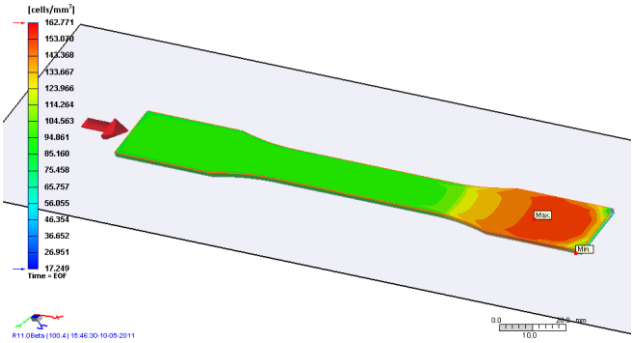

Fig. 4 Cell density distribution along center section of sample for 0.24 wt% N_2 SCF dissolved in PP. (Legend scale is 17 ~ 163 cells/mm^3)

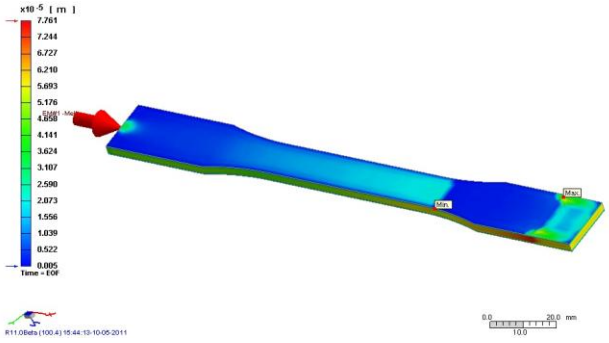

Fig. 5 Cell radius distribution of sample surface for 0.24 wt% N_2 SCF dissolved in PP. (Legend scale is from 0.05~77.61 μ m)

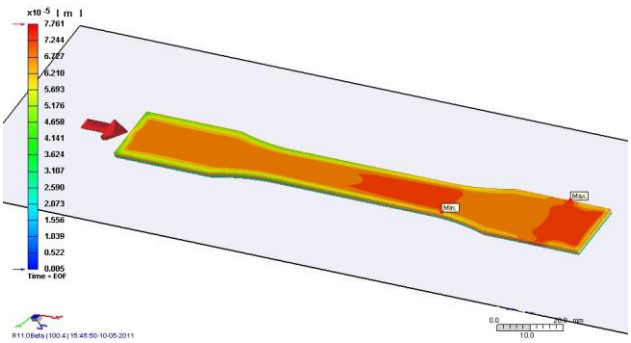

Fig. 6 Cell radius distribution along center section of sample for 0.24 wt% N_2 SCF dissolved in PP. (Legend scale is from 0.05~77.61 μ m)

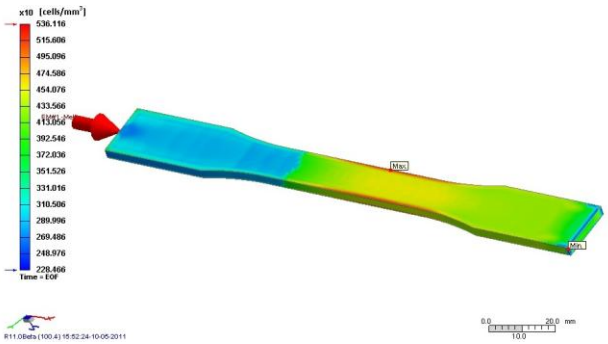

Fig. 7 Cell density distribution of sample surface for 0.57 wt% N_2 SCF dissolved in PP. (Legend scale is 2.28×10^3 ~ 5.36×10^3 cells/mm^3)

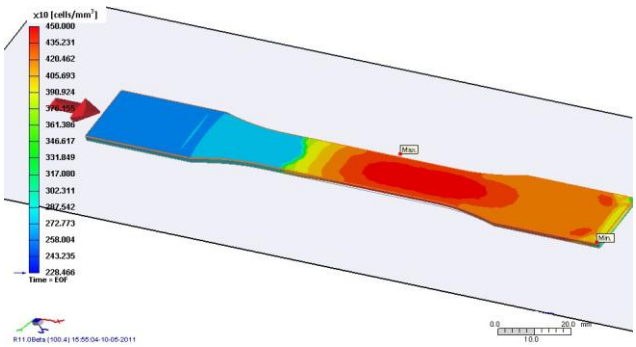

Fig. 8 Cell density distribution along center section of sample for 0.57 wt% N_2 SCF dissolved in PP. (Legend scale is 2.28×10^3 ~ 4.50×10^3 cells/mm^3)

Fig. 9 Cell radius distribution of sample surface for 0.57 wt% N_2 SCF dissolved in PP. (Legend scale is 3.03 ~ 32.38 μ m)

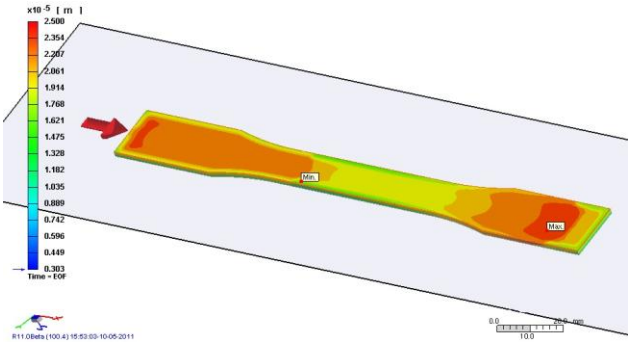

Fig. 10 Cell radius distribution along center section of sample for 0.57 wt% N_2 SCF dissolved in PP. (Legend scale is 3.03 ~ 32.38 μ m)

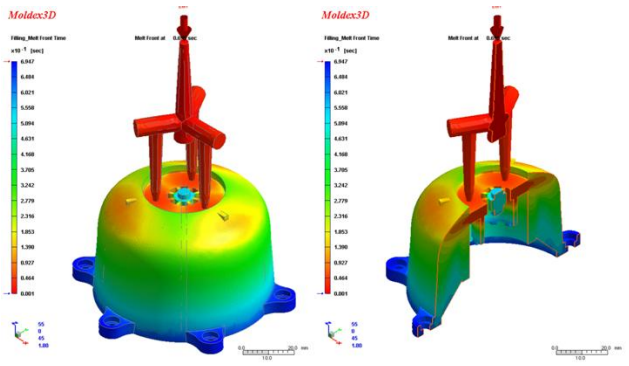

Fig. 11 Melt front time of microcellular injection molding. (Legend scale is 0.001 ~ 6.947x10^{-1} sec)

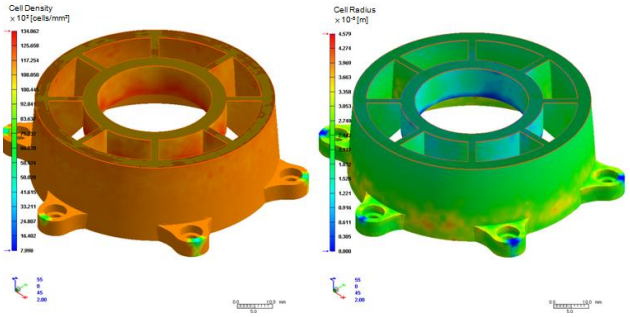

Fig. 12 Cross section of cell density distribution (left) and cell radius distribution (right) of molded part in z direction. (Legend scale: Left is 7.998 ~ 1.341x10^4cells/mm^3; Right: is 0 ~ 45.79μ m)

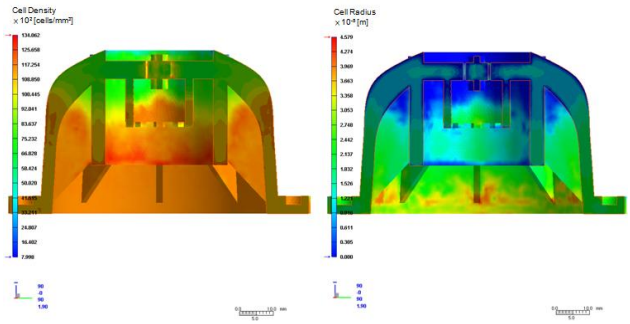

Fig. 13 Cross section of cell density distribution (left) and cell radius distribution (right) of molded part in x direction. (Legend scale: Left is 7.998 ~ 1.341x 10^4cells/mm^3; Right is 0 ~ 45.79μ m)

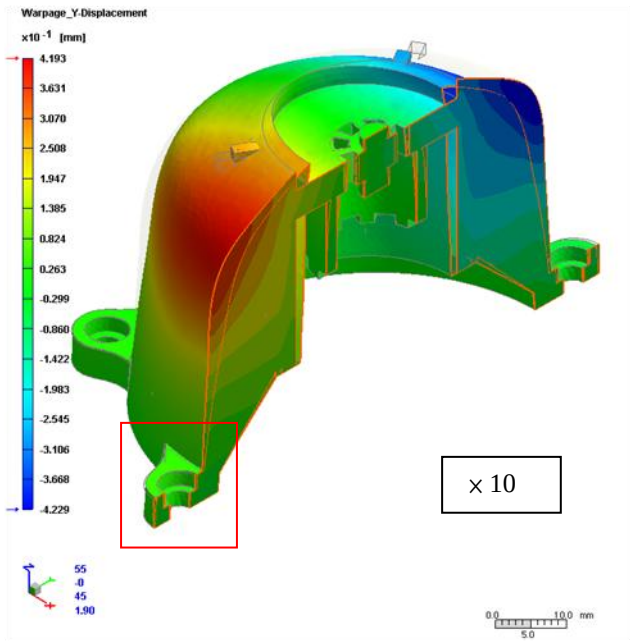

Fig. 14 Y-direction displacements of microcellular injection molded part. (Legend scale: -0.4229 ~ 4.193 mm)

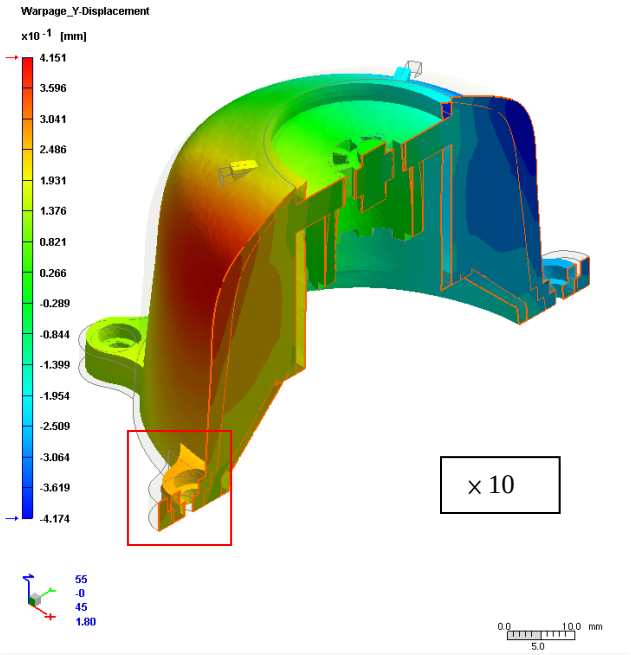

Fig. 15 Y-direction displacements of conventional injection molded part. (Legend scale: -0.4174 ~ 4.151 mm)